Nonlinear fastest growing perturbation and the first kind of predictability

MU Mu (穆 穆) & WANG Jiacheng (王家城)

LASG, Institute of Atmospheric Physics, Chinese Academy of Sciences, Beijing 100029, China
Correspondence should be addressed to Mu Mu (email: mumu@lasg.iap.ac.cn)

Received July 20, 2001

Abstract Nonlinear fastest growing perturbation, which is related to the nonlinear singular vector and nonlinear singular value proposed by the first author recently, is obtained by numerical approach for the two-dimensional quasigeostrophic model in this paper. The difference between the linear and nonlinear fastest growing perturbations is demonstrated. Moreover, local nonlinear fastest growing perturbations are also found numerically. This is one of the essential differences between linear and nonlinear theories, since in former case there is no local fastest growing perturbation. The results show that the nonlinear local fastest growing perturbations play a more important role in the study of the first kind of predictability than the nonlinear global fastest growing perturbation.

Keywords: singular vector, singular value, nonlinear, predictability.

In the research of atmospheric and oceanic sciences, the fastest growing perturbation plays an important role[1—4]. Usually, it is assumed that the perturbation is small enough such that its evolution can be governed approximately by the tangent linear model (TLM), and the forward propagator can be expressed as a matrix, so the linear fastest growing perturbation is the singular vector corresponding to the maximum singular value of the matrix. This linear theory of the fastest growing perturbation is widely used both in the theoretical study and in the numerical weather prediction (e.g. the ensemble forecast[5—8]). However, it is well known that the motion of the atmosphere or the ocean is governed by nonlinear systems, and the validity of the linear approximation should be investigated. The results of some researches show that it is necessary to deal with the nonlinear models themselves rather than the linear ones[9—11].

In ref. [12], a new concept of nonlinear singular value (NSVA) and nonlinear singular vector (NSV) is introduced, which is a natural generalization to the classical linear singular value (LSVA) and linear singular vector (LSV). The maximum NSVA of the corresponding NSV represents the growing rate of the fastest growing perturbation of the nonlinear model without linearizing the governing equations. The general idea of this approach is also demonstrated by a simple two-dimensional quasigeostrophic model in the atmospheric and oceanic sciences[12].

This paper is the second serial study on the NSAV and NSV following ref. [12]. By solving an optimization problem, the NSVA and NSV of the two-dimensional quasigeostrophic model are captured numerically. The difference between LSV and NSV is demonstrated. The local fastest

growing perturbations resulting from the nonlinearity of the model are found. The numerical approach also verifies the theoretical result that in the linear theory of singular vectors there exists no local fastest growing perturbation. Besides, the importance of the local fastest growing perturbations to the research of the first kind of predictability, which is related to the uncertainty caused by the initial errors, is also investigated.

1 Model and algorithm

Determination of the nonlinear fastest growing perturbation of models in the atmospheric or the oceanic dynamics usually results in nonlinear optimization problems of high dimension. It is too difficult to obtain its analytical solutions. Hence we adopt numerical approach. As the first step, we investigate the nonlinear fastest growing perturbation of two-dimensional quasigeostrophic model. The nondimensional governing equation is as follows:

$$\begin{cases} \dfrac{\partial P}{\partial t} + \partial(\Phi, P) = f, \\ P = \nabla^2 \Phi - F\Phi + f_0 + \dfrac{f_0}{H} h_s, \qquad \text{in} \quad \Omega \times [0,\ T], \\ \Phi\,|_{t=0} = \Phi_0, \end{cases} \tag{1.1}$$

where P is the potential vorticity, Φ the stream function, f the external forcing, F the Planetary Froude number, f_0 the Coriolis parameter, H the characteristic vertical depth and h_s the topography. The Jacobian operator $\partial(\Phi,\ P) = \Phi_x P_y - \Phi_y P_x$. For simplicity, $f = 0$, $\Omega = [0,\ X] \times [0,\ Y]$ with double periodical boundary condition. For fixed $T > 0$ and initial condition $\Phi\,|_{t=0} = \Phi_0$. The propagator M is well-defined, i.e. $\Phi(x, y, T) = M(\Phi_0)$ is the solution of (1.1) at time T (Mu and Zeng, 1991)[13].

Let Ψ_0 be the initial value of stream function Ψ, to which ψ_0 is the initial perturbation, so the solutions of (1.1) with initial value Ψ_0 and $\Phi_0 = \Psi_0 + \psi_0$ are

$$\Psi_T = M(\Psi_0), \qquad \Phi_T = M(\Psi_0 + \psi_0). \tag{1.2}$$

In the research of predictability, energy norm is widely employed[4,7,8], which is defined as follows:

$$\|\phi\|^2 = \int_\Omega (|\nabla \phi|^2 + F|\phi|^2)\mathrm{d}x\mathrm{d}y, \tag{1.3}$$

where ϕ is the stream function. The nonlinear fastest growing perturbation, which is also called the first nonlinear singular vector, ψ_0^*, is the maximum of functional

$$J(\psi_0) = \frac{\|\Phi_T - \Psi_T\|^2}{\|\psi_0\|^2} = \frac{\|M(\Psi_0 + \psi_0) - M(\Psi_0)\|^2}{\|\psi_0\|^2}. \tag{1.4}$$

The first nonlinear singular value is

$$\lambda = (J(\psi_0^*))^{1/2}. \tag{1.5}$$

According to refs.[12, 13], ψ_0^* and λ are well-defined.

To capture the maximum of $J(\psi_0)$, we calculate the minimum of

$$J_1(\psi_0) = \frac{1}{J(\psi_0)} = \frac{\|\psi_0\|^2}{\|M(\Psi_0+\psi_0) - M(\Psi_0)\|^2}. \tag{1.6}$$

The first variation of $J_1(\psi_0)$ is

$$\begin{aligned}\delta J_1(\psi_0) = 2(((-\nabla^2 + F)\psi_0,\ \delta\psi_0)\|M(\Psi_0+\psi_0) - M(\Psi_0)\|^2 \\ -((-\nabla^2 + F)(M(\Psi_0+\psi_0) - M(\Psi_0)),\ \mathrm{M}(\Psi_0+\psi_0)\delta\psi_0)\|\psi_0\|^2) \\ /\|M(\Psi_0+\psi_0) - M(\Psi_0)\|^4,\end{aligned} \tag{1.7}$$

where $\mathrm{M}(\Psi_0+\psi_0)$ is the tangent linear approximation of propagator M at $\Psi_0+\psi_0$.

Let M^* be the adjoint operator of M, we have

$$\begin{aligned}\delta J_1(\psi_0) = 2(((-\nabla^2 + F)\psi_0,\ \delta\psi_0)\|M(\Psi_0+\psi_0) - M(\Psi_0)\|^2 \\ -(\mathrm{M}^*(\Psi_0+\psi_0)(-\nabla^2 + F)(M(\Psi_0+\psi_0) - M(\Psi_0))\delta\psi_0)\|\psi_0\|^2) \\ /\|M(\Psi_0+\psi_0) - M(\Psi_0)\|^4.\end{aligned} \tag{1.8}$$

To obtain the nonlinear fastest growing perturbation numerically, we need two main numerical steps, i.e. the discretization of operator M and optimization of functional $J_1(\psi_0)$. In our numerical approach, Arakawa finite difference scheme[14] is used to discretize the Jacbian operator. The temporal discretization is Adamas-Bashforth scheme, stream function Φ is treated as unknown term, and the potential vorticity P is calculated by using the second equation of (1.1). The familiar five-point difference scheme is employed to discretize the Laplacian operator.

The optimization algorithm is limited memory BFGS method[15], which is an extension of the conjugate gradient method. This method is suitable for large scale optimization problems because the amount of storage required by the algorithm and thus the cost of the iteration can be controlled by the user. In the research of predictability, data assimilation and ensemble forecast, this method has been successfully applied to solving the related optimization problems with high dimensions. The details of this algorithm can be found in ref. [15].

2 Numerical results

In this section, we present the results of our numerical experiments. Three cases of different basic flows and topographies are chosen to calculate the nonlinear fastest growing perturbation. In some cases, the nonlinear fastest growing perturbations are almost the same as the LSV because the energy norm of the nonlinear fastest growing perturbation is small enough such that TLM holds. On the other hand, some numerical results show that besides the first nonlinear fastest growing perturbation, which is the global maximum of the functional, other local nonlinear fastest

growing perturbations are found, due to the nonlinearity of the model.

We take the space domain $\Omega=[0, 6.4]\times[0, 3.2]$, which corresponds to the dimensional case [0, 6400 km]×[0, 3200 km], the parameters $F = 0.1$, $f_0 = 10$, $1/H = 1.0$, the space step $d = 0.2$ corresponding dimensional case 200 km and the time step $t = 0.006$ corresponding $t = 10$ min.

2.1 Experiment 1

The first basic flow is $\Psi_0 = a\times 0.1\times\sin(2\pi x/6.4)+b\times\sin(2\pi y/3.2)+c$, where $a = 1.1852$, $b = 0.3259$, $c = -45.3019$. This is a steady state. The total energy norm of Ψ_0 is 65.5226, and the topography $h_s = 0.1\times\sin(2\pi x/6.4)+1.0\times\sin(2\pi y/3.2)$. We fix $T = 720$, 1008, 1440 steps (corresponding to 5, 7 and 10 days respectively). The results of this experiment are summarized in table 1, where $\|\psi_0^1\|$ is the energy norm of the first NSV. To investigate its effect on the predictability, $\|\psi_N^1(T)\|$ and $\|\psi_L^1(T)\|$, which are the norms of its nonlinear and linear evolutions respectively, are presented for 5, 7 and 10 days. λ_L is the first LSVA, obtained by replacing the nonlinear propagator M with its TLM approximation M in (1.4). λ^1 and λ_L represent the nonlinear fastest growing rate and the linear fastest growing rate of the initial perturbations, which are the measures of the nonlinear predictability and linear predictability respectively.

It follows from table 1 that the energy of the first NSV, i.e. $\|\psi_0^1\|$, is very small, and its nonlinear and linear evolutions have no remarkable difference for 5 days. In fact, in this case we can show that ψ_0^1 is almost the same as the first linear singular vector, and λ_L^1 is an approximation to the first nonlinear singular value with high accuracy. To demonstrate this, we define the functional

$$J_L(\psi_0)=\frac{\|\psi_L(T)\|^2}{\|\psi_0\|^2}, \tag{2.1}$$

where $\psi_L(T)$ is obtained by integrating the corresponding TLM with initial value ψ_0. Since ψ_0^1 is very small, we can assume that in a ball with center at Ψ_0, which is denoted by D, the TLM approximation holds, and $\Psi_0+\psi_0^1$ belongs to D. Now for any ψ_0 that $\Psi_0+\psi_0$ belongs to D, we have $J(\psi_0)\leqslant J(\psi_0^1)$. The validity of TLM in D yields that $J_L(\psi_0)\leqslant J_L(\psi_0^1)$ holds approximately. Now if ψ_0 is so large that $\Psi_0+\psi_0$ does not belong to D, we can choose a constant α large enough such that $\Psi_0+\psi_0/\alpha$ belongs to D, hence $J_L(\psi_0)=J_L(\psi_0/\alpha)\leqslant J_L(\psi_0^1)$ holds approximately. This yields the above conclusion. On the other hand, we also employed numerical approach to find out the first LSV and the corresponding first LSVA, and the results are shown in the last row of table 1, which does verify our conclusion.

From table 1 we find out that with the time increasing from 5 days to 7 days (10 days), λ^1 increases too, and the TLM is not a good approximation. In this case there exists a considerable dif-

ference between linear and nonlinear SVs, and the corresponding SVAs.

Table 1 Results of Exp.1

	5 days	7 days	10 days
λ^1	4.3760	6.5144	10.0002
$\left\|\psi_0^1\right\|$	1.4277E-4	0.5218E-1	3.8812E-2
$\dfrac{\left\|\psi_0^1\right\|}{\left\|\Psi\right\|}$	2.1790E-6	7.9637E-4	5.9235E-4
$\left\|\psi_N^1(T)\right\|$	6.2478E-4	3.3992E-1	3.8812E-1
$\left\|\psi_L^1(T)\right\|$	6.2074E-4	3.2574E-1	3.2630E-1
$\dfrac{\left\|\psi_L^1(T)\right\|}{\left\|\psi_0^1\right\|}$	4.3477	6.2426	8.4069
λ_L	4.3494	6.3808	9.3611

Fig. 1 is the first NSV for 7 days, figs. 2, 3 and 4 are the first NSV, its linear evolution and nonlinear evolution for 10 days respectively.

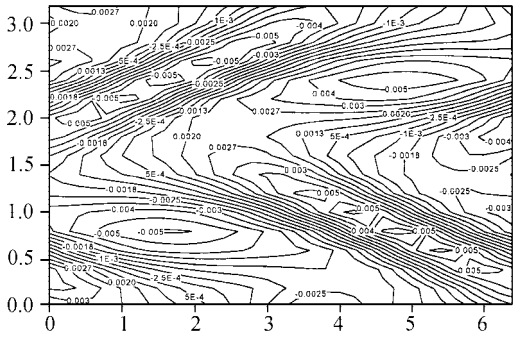

Fig. 1. The first NSV for 7 days, Exp. 1.

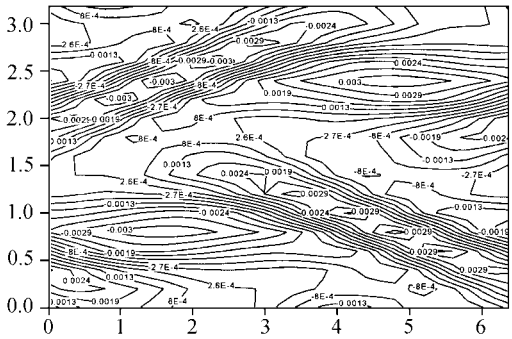

Fig. 2. The first NSV for 10 days, Exp. 1.

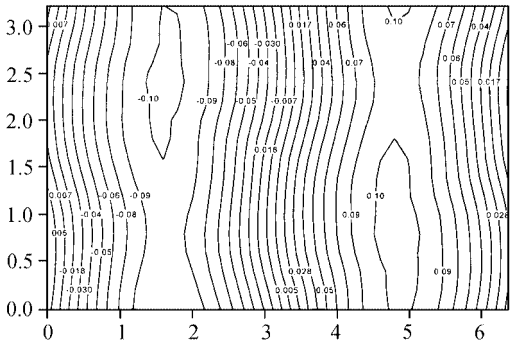

Fig. 3. The linear evolution of the first NSV after 10 days, Exp. 1.

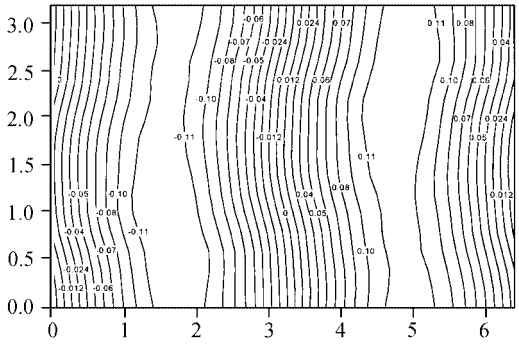

Fig. 4. The nonlinear evolution of the first NSV after 10 days, Exp. 1.

It follows from table 1, figs. 1 and 2 that although the energy norm of the first NSVs for 5, 7 and 10 days increases with time, the patterns of these NSVs are quite similar. On the other hand,

there is no such similarity among the global and local maxima in the following experiments, which will be discussed later.

2.2 Experiment 2

The second experiment is for the basic flow $\Psi_0 = 1.0 \times (\sin(2\pi y/3.2) + 0.25)$, which is also a steady state, the topography $h_s = 1.0 \times \sin(2\pi\, y\, /3.2)$, $1/H = 0.35$, and the other parameters are the same as the first experiment. The energy norm of the basic flow is $\|\Psi_0\| = 6.3363$.

For T=720 steps (corresponding to 5 days), we find 1 global and 2 local maxima of functional $J(\psi_0)$. The detailed information about these 3 global and local nonlinear fastest growing perturbations is shown in table 2.

Table 2 The 3 global and local maxima for 5 days, Exp. 2

	$i = 1$	$i = 2$	$i = 3$
λ_1^i	9.1171	6.2344	5.5339
$\|\psi_{0i}^1\|$	2.0274E-4	8.9496E-1	1.3910
$\|\psi_{0i}^1\|/\|\Psi\|$	3.1998E-5	0.1412	0.2195
$\|\psi_{Ni}^1(T)\|$	1.8485E-3	5.5796	7.6971
$\|\psi_{Li}^1(T)\|$	1.8485E-3	1.3391	3.2895
$\|\psi_{Li}^1(T)\|/\|\psi_{0i}^1\|$	9.1171	1.4963	2.3650
λ_L	9.1171	—	—

For T=1008 steps (corresponding to 7 days), we find 1 global and 4 local maxima of functional $J(\psi_0)$, and the detailed information about these 5 global and local nonlinear fastest growing perturbations is shown in table 3.

Table 3 The 5 global and local maxima for 7 days, Exp. 2

	$i = 1$	$i = 2$	$i = 3$	$i = 4$	$i = 5$
λ_1^i	10.0618	7.5523	7.3327	5.3232	5.1484
$\|\psi_{0i}^1\|$	5.1058E-5	6.4011E-1	5.1695E-1	2.1387	2.3723
$\|\psi_{0i}^1\|/\|\Psi\|$	8.0579E-6	1.0102E-1	8.1585E-2	0.3375	0.3744
$\|\psi_{Ni}^1(T)\|$	5.1373E-4	4.8343	3.7907	11.3849	12.2139
$\|\psi_{Li}^1(T)\|$	5.1373E-4	1.0786	1.8972	3.0900	2.8588
$\|\psi_{Li}^1(T)\|/\|\psi_{0i}^1\|$	10.0618	1.6850	3.6700	1.4448	1.2050
λ_L	10.0618	—	—	—	——

Fig. 5 is ψ_{01}^1, the global nonlinear fastest growing perturbation. Figs. 6, 7, 8 and 9 are the four local nonlinear fastest growing perturbations ψ_{0i}^1 ($i = 2,\cdots, 5$) for 7 days.

The above numerical results show a distinct difference between linear and nonlinear approaches of the fastest growing perturbations, that is, the existence of local maximum in the nonlinear case. It is worthwhile to point out that in the linear case there exists only global maxi-

mum, but no local maximum, which can be proved theoretically. Our numerical result does verify this. On the other hand, it is reasonable to expect that in the nonlinear case there exists local maximum due to the nonlinearity. Since the corresponding optimization problem is of high dimension, usually the theoretical proof of this is beyond our grasp. With the numerical approach, we do find out the local maxima.

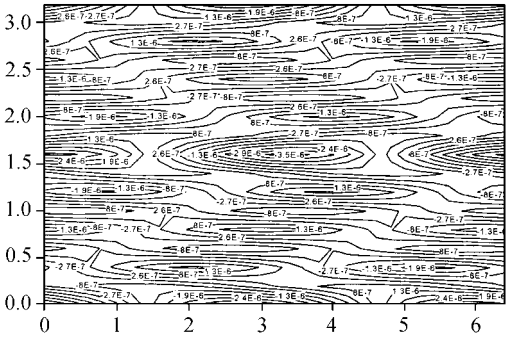

Fig. 5. ψ_{01}^{1} for 7 days, Exp. 2.

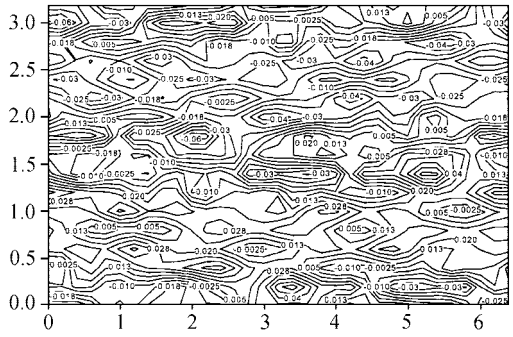

Fig. 6. ψ_{02}^{1} for 7 days, Exp. 2.

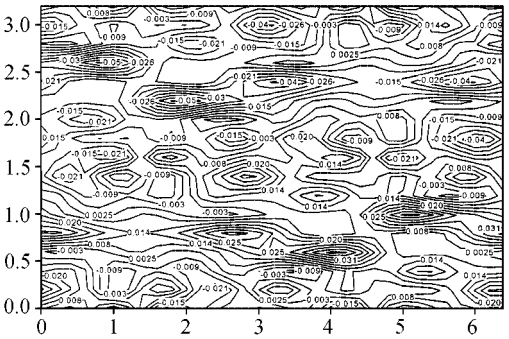

Fig. 7. ψ_{03}^{1} for 7 days, Exp. 2.

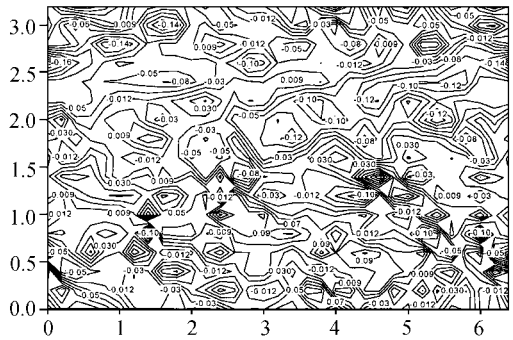

Fig. 8. ψ_{04}^{1} for 7 days, Exp. 2.

Now that we have found more than one maximum of functional $J(\psi_0)$, which one is more important in the study of predictability, NSV or other local fastest growing perturbations? Since the energy norm is one of the useful measures in the study of predictability, let us consider their energy. The energy norm of NSV (ψ_{01}^{1}) is much smaller than that of ψ_{02}^{1}. Although its corresponding NSVA λ_1^1 is larger than λ_1^2, the nonlinear evolution of ψ_{01}^{1} is

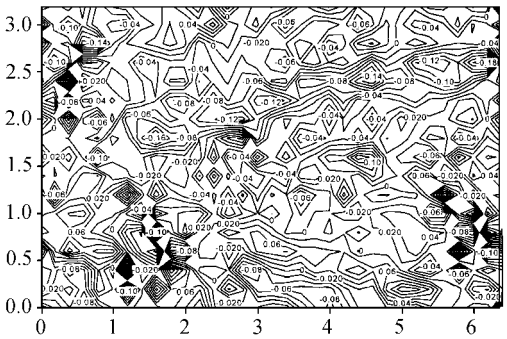

Fig. 9. ψ_{05}^{1} for 7 days, Exp. 2.

also smaller than the nonlinear evolution of ψ_{02}^1 in terms of energy norm.This is clearly demonstrated by the quantities of $\|\psi_{Ni}^1(T)\|$ in the above tables. Hence, the effect of ψ_{02}^1 on the predictability is greater than that of ψ_{01}^1.

Of course, we may argue that multiplying an LSV by a constant yields another LSV. One could always multiply ψ_{01}^1 by a constant such that the resulting LSV plays an important role as ψ_{02}^1. For example, let

$$\tilde{\psi}_{01} = \frac{\|\psi_{02}^1(T)\|}{\lambda_1^1\|\psi_{01}^1\|}\psi_{01}^1, \tag{2.2}$$

thus

$$\|\tilde{\psi}_{01L}(T)\| = \lambda_1^1\|\tilde{\psi}_{01}\| = \|\psi_{02}^1(T)\|. \tag{2.3}$$

Now, one question should be investigated, that is, how about the validity of TLM for this scaled $\tilde{\psi}_{01}$?

With this aim, taking $\tilde{\psi}_{01}$ as the initial value, integrating nonlinear model (NM) and (TLM) respectively, we obtain $\tilde{\psi}_{01L}(T)$ and $\tilde{\psi}_{01N}(T)$.

Fig. 10 is the linear evolution of $\tilde{\psi}_{01}$ after 7 days, $\|\tilde{\psi}_{01L}(T)\| = 4.8342$, $\|\tilde{\psi}_{01L}(T)\|/\|\Psi\| = 0.7629$, fig. 11 is the nonlinear evolution of $\tilde{\psi}_{01}$ after 7 days, $\|\tilde{\psi}_{01N}(T)\| = 2.2551$, $\|\tilde{\psi}_{01N}(T)\|/\|\Psi\| = 0.3559$. It is easily seen that the linear evolution and the nonlinear evolution of $\tilde{\psi}_{01}$ are quite different, the former is a regular meridional flow, but for the latter, the zonal component of the flow becomes considerably strong. Consequently, TLM cannot be used to approximate the evolution of $\tilde{\psi}_{01}$.

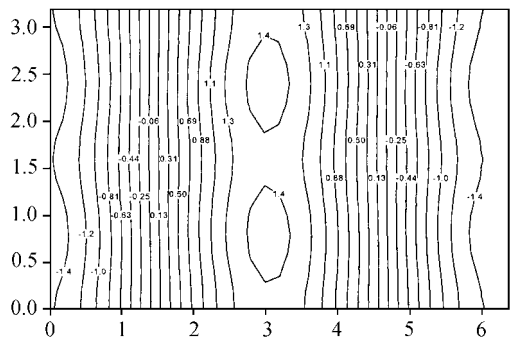

Fig. 10. The linear evolution of $\tilde{\psi}_{01}$ after 7 days, Exp. 2.

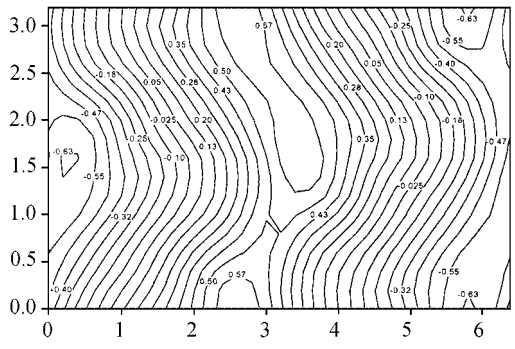

Fig. 11. The nonlinear evolution of $\tilde{\psi}_{01}$ after 7 days, Exp. 2.

We also investigate the cases of ψ_{0i}^1 (i = 3, 4, 5), and find that the local maxima ψ_{02}^1 and others really play a more important role than the global maximum, due to the fact that TLM can-

not be used for the scaled LSVs. We have mentioned in the above subsection that there exists a similarity among the NSVs for different time periods, but for the global and local maxima for a given time period, there is no such similarity. Besides, it follows from the figures that for the global and local maxima with a fixed period time, the larger the energy of the maximum, the smaller the wavelength of the flow. This suggests that to reduce the uncertainty of the numerical forecast, attention should be paid to the errors with short wavelength.

2.3 Experiment 3

The above two experiments are concerned with the steady basic flows. In this experiment we investigate a more realistic case of unsteady basic flow, which is given by integrating the initial state $\Psi_0 = 1.0 \times (\sin(2\pi y/3.2) + 0.25) + 0.1 \times \sin(2\pi x/6.4)$. The topography $h_s = 1.0 \times \sin(2\pi y/3.2)$, the other parameters are the same as the second experiment. The energy norm of the initial basic flow $\|\Psi_0\| = 6.3449$.

For T = 720 steps (corresponding to 5 days), we find 1 global and 2 local maxima of functional $J(\psi_0)$, which is the same as the second experiment. The detailed information about these 3 global and local nonlinear fastest growing perturbations is shown in table 4.

Table 4 The 3 global and local maxima for 5 days, Exp. 3

	i = 1	i = 2	i = 3
λ_i^1	9.1555	6.2607	5.3523
$\|\psi_{0i}^1\|$	4.7677E-4	8.7499E-1	1.7423
$\|\psi_{0i}^1\|/\|\Psi(0)\|$	7.5142E-5	1.3790E-1	0.2746
$\|\psi_{Ni}^1(T)\|$	4.3651E-3	5.4780	9.3256
$\|\psi_{Li}^1(T)\|$	3.6321E-3	1.0867	2.7290
$\|\psi_{Li}^1(T)\|/\|\psi_{0i}^1\|$	7.6181	1.2419	1.5663
λ_L	8.8744	—	—

For T = 1008 steps (corresponding to 7 days), we find 1 global and 4 local maxima of functional $J(\psi_0)$. The detailed information about these 5 global and local nonlinear fastest growing perturbations is shown in table 5.

Table 5 The 5 global and local maxima for 7 days, Exp. 3

	i = 1	i = 2	i = 3	i = 4	i = 5
λ_i^1	10.1399	7.6248	7.6156	6.2984	5.8797
$\|\psi_{0i}^1\|$	1.2619E-2	4.5164E-1	6.1295E-1	1.1974	1.5408
$\|\psi_{0i}^1\|/\|\Psi(0)\|$	1.9889E-3	7.1181E-2	9.6605E-2	1.8872E-1	2.4284E-1
$\|\psi_{Ni}^1(T)\|$	1.2796E-1	3.4436	4.6680	7.5418	9.0592
$\|\psi_{Li}^1(T)\|$	8.0268E-2	5.7729E-1	1.5745	1.9155	2.0573
$\|\psi_{Li}^1(T)\|/\|\psi_{0i}^1\|$	6.3607	1.2782	2.5687	1.5997	1.3352
λ_L	9.5032	—	—	—	——

Fig. 12 is ψ_{01}^1, the global nonlinear fastest growing perturbation, figs. 13, 14, 15 and 16 are the local nonlinear fastest growing perturbations ψ_{0i}^1 (i = 2, ⋯, 5) for 7 days.

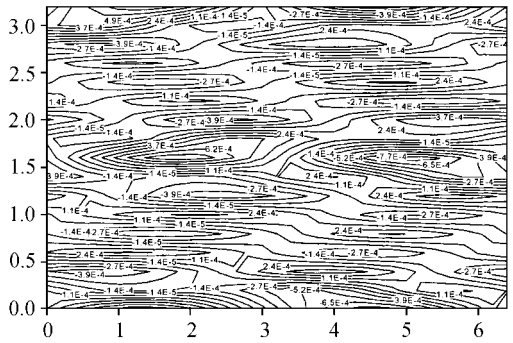

Fig. 12. ψ_{01}^1 for 7 days, Exp. 3.

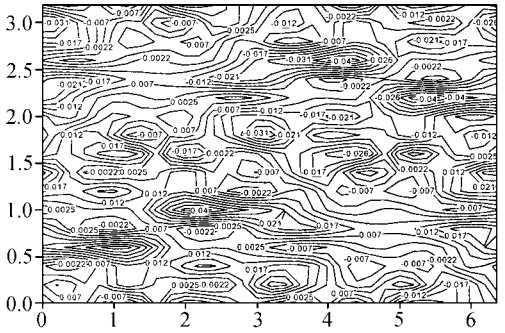

Fig. 13. ψ_{02}^1 for 7 days, Exp. 3.

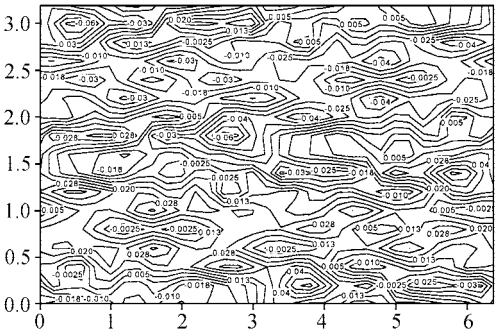

Fig. 14. ψ_{03}^1 for 7 days, Exp. 3.

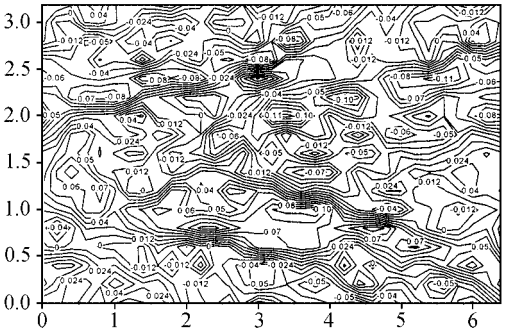

Fig. 15. ψ_{04}^1 for 7 days, Exp. 3.

Similarly to the second experiment, we find more than one local fastest growing perturbation due to the nonlinearity. The global and local maxima possess same properties as in the second experiment. Particularly, the energy norm of NSV (ψ_{01}^1) is small enough such that it is almost the same as the LSV. On the other hand, ψ_{0i}^1, i = 2,⋯are much larger than NSV ψ_{01}^1 in terms of energy norm, and their nonlinear evolutions are also larger than the NSV's. Consequently the local fastest growing perturbations play more important roles than the global one. If ψ_{01}^1 is scaled such that its linear evolution equals the nonlinear evolution of ψ_{02}^1 (c.f. (2.2)), then TLM is not a good approximation to capture the

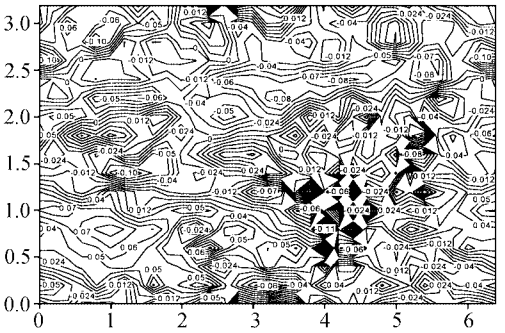

Fig. 16. ψ_{05}^1 for 7 days, Exp. 3.

nonlinear evolution of the scaled ψ_{01}^{1}. The detailed arguments are omitted here for simplicity.

3 Conclusion and discussion

In this paper, the NSVAs and NSVs of the two-dimensional quasigeostrophic model are obtained by solving the corresponding optimization problem numerically, which follows the theoretical research on NSVA and NSV in ref. [12]. The main results are as follows:

First, if the first NSV is small enough such that in a neighborhood of the basic state, the corresponding TLM holds, and the first NSV belongs to this neighborhood too, then the first NSV is almost the same as the first LSV, and the first NSVA is equal to the first LSVA approximately. On the other hand, when the first LSV is not so small, and the related TLM is not a good approximation to the original nonlinear model, then there exists a considerable difference between the first NSV (resp. NSVA) and the first LSV (resp. LSVA), which suggests that we should investigate the NSV and NSVA rather than LSV and LSVA.

Secondly, for some kinds of basic states, we only find a global maximum of the functional, which is the first NSV. But for some kinds of basic states, there exist local maxima of the functional besides the global maximum. There is no such phenomenon in the case of LSVs and LSVAs due to the linearity of the corresponding TLM. These numerical results verify the linear theory of singular vectors, and also demonstrate the complexity caused by nonlinearity.

Thirdly, it is found that the local maxima usually possess larger energy norm with shorter wavelength comparing to the global maximum. Although the growing rate of it is relatively smaller than the first NSVA, the evolution of the local maxima at the end of time interval, in terms of the energy norm, is considerably greater than that of the first NSV. This suggests that to reduce the uncertainty caused by the initial errors, we should pay more attention to the initial errors possessing the patterns similar to the local maximum, which is of short wavelength.

The above results are obtained for a relatively simple two-dimensional quasigeostrophic model, and only the case of energy norm is investigated, though it is one of the widely used measures in the research of predictability. Concerning the further work, the problem whether the results are model-dependent should be investigated and more realistic models in the atmospheric or oceanic sciences should be considered. For example, a baroclinic quasigeostrophic model, and the simple Zebiak-Cane model of ENSO could be taken into account as the first step[7,8]. Moreover, other norms, e.g., the potential enstrophy, could be adopted to measure the evolution of the initial errors, and to investigate the related NSVs and NSVAs.

For more realistic cases in the numerical weather forecast and climate prediction, we would like to point out that there exists an essential difference between LSVs and NSVs, i.e. the former represents the optimal growing direction due to the linearity, and the latter only stands for a kind of initial pattern growing with maximum rate, which is not a direction because of nonlinearity. Considering that although the precise information of the initial errors is not available, we have some statistical information on the initial errors in practice. The results in this paper suggest that it

is worthwhile to investigate the nonlinear fastest growing perturbation of some kinds of objective functionals with constrained conditions, which represents the statistical information of initial errors. The roles of such NSVs and NSVAs in predictability are of great importance to further research.

Acknowledgements This work was supported by the National Key Basic Research Project, "Research on the Formation Mechanism and Prediction Theory of Severe Synoptic Disasters in China" (Grand No. G1998040910), the National Natural Science Foundation of China (Grand Nos. 49775262 and 49823002) and the Chinese Academy of Sciences (Grand No. KZCX 2-208).

References

1. Lorenz, E. N., A study of the predictability of a 28-variable atmospheric model, Tellus, 1965, XVII 3: 321.
2. Palmer, T. N., Buizza, R., Molteni, F. et al., Singular vectors and the predictability of weather and climate, Phil. Trans. R. Soc. Lond. A., 1994, 348: 459.
3. Farrell, B. F., Small error dynamics and the predictability of flows, J. Atmos. Sci., 1990, 47: 2409.
4. Roberto Buizza, Optimal perturbation time evolution and sensitivity of ensemble prediction to perturbation amplitude, Q. J. R. Meteorol. Soc., 1995, 121: 1705.
5. Molteni, F., Palmer, T. N., Predictability and finite-time instability of the northern winter circulation, Q. J. R. Meteorol. Soc., 1993, 119: 269.
6. Thompson, C. J., Initial conditions for optimal growth in a coupled ocean-atmosphere model of ENSO, J. Atmos. Sci., 1998, 55: 537.
7. Xue, Y., Cane, Y. M. A., Zebiak, S. E., Predictability of a coupled model of ENSO using singular vector analysis, Part I: Optimal growth in seasonal background and ENSO cycles, Mon. Wea. Rev., 1997, 125: 2043.
8. Xue, Y., Cane, Y. M. A., Zebiak, S. E., Predictability of a coupled model of ENSO using singular vector analysis, Part II: Optimal growth and forecast skill, Mon. Wea. Rev., 1997, 125: 2057.
9. Lacarra, J. F., Talagrand, O., Short-range evolution of small perturbation in a baratropic model, Tellus, 1998, 40A: 81.
10. Tanguay, M., Bartello, P., Gauthier, P., Four-dimensional data assimilation with a wide range of scales, Tellus, 1995, 47A: 974.
11. Mu Mu, Guo Huan, Wang Jiafeng et al., The impact of nonlinear stability and instability on the validity of the tangent linear model., Adv. Atmos. Sci., 2000, 17: 375.
12. Mu Mu, Nonlinear singular vectors and nonlinear singular values, Science in China, Ser. D, 2000, 43: 375.
13. Mu Mu, Zeng Qingcun, New development on existence and uniqueness of solutions to some models in atmospheric dynamics, Adv. Atmos. Sci., 1991, 8: 383.
14. Liao Dongxian, Wang Liangming, Principle of Numerical Weather Forecasting and Its Applications (in Chinese), Beijing: Meteorology Press, 1986.
15. Dong, C. L., Jorge Nocedal, On the limited memory BFGS method for large scale optimization, Mathematical Programming, 1989, 45: 503.